Journal of Sound and Vibration (2000) **237**(1), 119–143
doi:10.1006/jsvi.2000.3023, available online at http://www.idealibrary.com on IDEAL®

THE FINITE ELEMENT METHOD FOR HYDROELASTIC INSTABILITY OF UNDERWATER TOWED CYLINDRICAL STRUCTURES

S. K. Bhattacharyya and C. P. Vendhan

Ocean Engineering Centre, Indian Institute of Technology, Madras 600036, *India*

and

K. Sudarsan

Naval Physical and Oceanographic Laboratory, Cochin 682021, *India*

(*Received* 4 *August* 1999, *and in final form* 28 *March* 2000)

The dynamics of underwater towing of flexible cylindrical structures belongs to the class of fluid–structure interaction problems commonly referred to as "cylinders in axial flow". The serious concern in such towing operations is the various types of hydroelastic instabilities exhibited by the structure at certain critical tow speeds. In practice, reliable prediction of tow configurations and stability characteristics of such towed systems can lead to optimum deployment of cable scope and control of tow speed. The present investigation is concerned with the development of a comprehensive linear finite element method for the dynamics of the flexible towed cylinder with focus on the stability behaviour. The finite element approximation is derived from a variational statement of the problem based on Hamilton's principle. The various structure- and fluid-related matrices as well as matrices resulting from boundary terms have been derived, resulting in a complex unsymmetric eigenvalue problem. Exhaustive validation and convergence studies show that the comparisons between finite element and analytical results are almost exact. Using the finite element code, the hydroelastic instability of a ship-towed array system has been analyzed. The effect of cable scope and shape of the downstream end on stability have been examined.

1. INTRODUCTION

The dynamics of a slender flexible (i.e., elastic) cylinder surrounded by a flowing fluid with constant velocity with the flow direction coinciding with the undisturbed centroidal axis of the cylinder is an established fluid–structure interaction problem which has a well-developed literature [1, 2]. Specifically, when the cylinder is towed underwater by a tow rope or is cantilevered with a drougue attached at the free end, the system has non-conservative end (or follower) forces as against no such force when both the ends of the cylinder are transversely restrained against displacement. This problem is of concern in the present investigation. A comprehensive theoretical model of this problem was presented in reference [3] within the framework of small amplitude motions (i.e., linear behavior) of the cylinder modelled by elementary (Euler–Bernoulli) beam theory, linearized hydrodynamic force models based on cross-flow principle and an uniform virtual mass of the cylinder over its entire length. The governing equation of motion is a single equation involving the transverse (i.e., lateral) displacement of the cylinder as the variable.

0022-460X/00/410119 + 25 $35.00/0

Two aspects, which significantly affect the instability behaviour of cantilevered and towed cylinders in axial flow, are the shape of the downstream end and the imposed tension at this end. The effect of the tapered end shape is incorporated by means of an empirical constant in a lumped end force term in the free end boundary condition. This shape can be looked upon, theoretically speaking, ranging from "fully streamlined" to "blunt". The end tension can always be lumped at the free end based upon the chosen hydrodynamic formulation or prescribed at the end if known from experimental data. The end shape constant however is difficult to ascertain experimentally and is usually adjusted to match theory with experiments. A blunt end as well as an end tension can vastly improve the stability of the system. These two effects therefore always merited extensive discussion in the literature.

The analytical solution methods used in the literature are the "beam eigenfunction expansion method" (BEEM) and the "power series method" (PSM). However, these methods cannot treat the problem of a string in axial flow, which represents a limiting case of flexible cylinder with zero flexural rigidity. For this case, treated in a few papers [4, 5], alternative analytical solutions which involve Bessel functions have been used.

Recently, a finite element method had been presented [6] to treat the "cylinder in axial flow" problem for cylinders with both ends supported. Therefore, towing problems, which involve the significant effect of the shapes of the up- and downstream ends, tow rope pull and drougue force at the downstream end on stability, cannot be solved by this method. In the present work, a finite element method is developed for such systems, which has not been hitherto attempted in the literature. This is done from the variational statement in the form of Hamilton's principle. The element matrices are obtained in closed form and the finite element system of equations is solved using the determinant search technique. The system with both ends supported becomes a special case of the present formulation.

In any practical problem of ship-towed cylindrical structure, which could be a seismic streamer, a sonar array or a flexible barge for liquid cargo transport, hydroelastic instability of any kind is detrimental to the safety and operability of the systems. Its prediction is therefore crucial in practice. Analytical methods cannot be used for these problems since they are based on an equilibrium configuration where the both the tow rope and the towed cylinder are assumed to be in a single horizontal line at all tow speeds, whereas in ship towing problem, the tow rope (from ship's winch to the towed cylinder at a certain depth below water surface) is not horizontal. Besides, the non-uniformity of elastic as well as hydrodynamic properties along the length is inevitable (in fact sometimes desirable by design, e.g., non-constant diameter arrays) defying analytical solution. Need to develop a finite element method is therefore obvious.

One of the earliest applications of the finite element method to non-conservative problems was devoted to stability of beams using Hamilton principle as basis and the dynamic criterion of stability [7]. A similar formulation was applied to the Beck problem [8]. There have been a few studies on the application of the finite element method to the non-conservative problem of pipes conveying fluids. In reference [9], the finite element method was applied to slender pipe conveying fluids. In reference [10], it was demonstrated that the formulation employing Timoshenko beam elements exhibited a good comparison with closed-form solution. In reference [11], the finite element method was employed to study the feedback control of cantilevered pipes aspirating fluid.

2. GOVERNING EQUATION

The derivation of the equation of motion is recapitulated in this section closely following the treatment in reference [3] before considering its variational form to facilitate the finite element approximation.

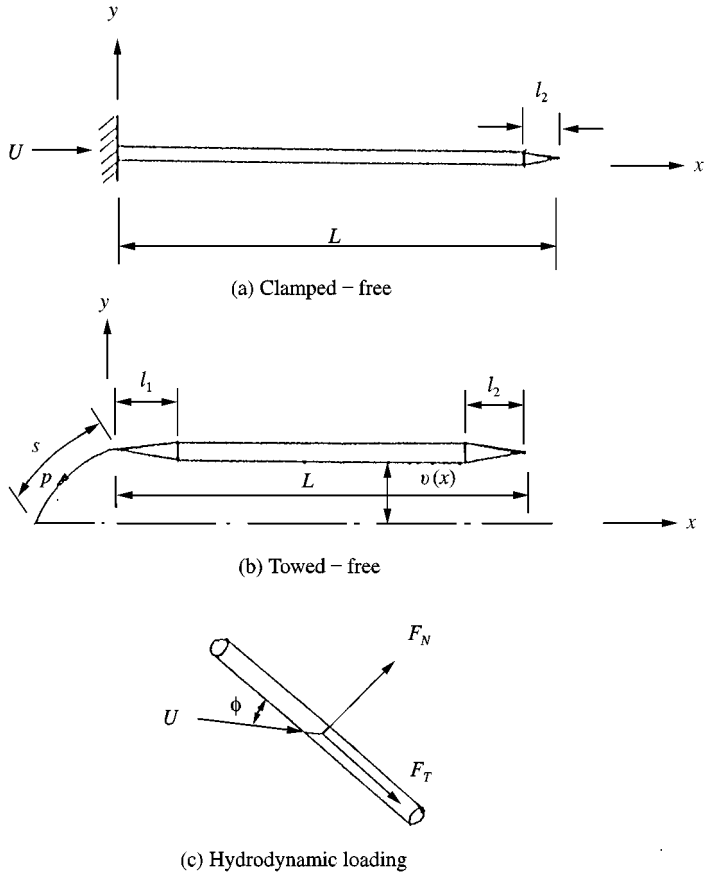

Figure 1. Definition sketches of the cylinder: (a) clamped–free; (b) towed–free; (c) hydrodynamic loading.

Consider a flexible, long circular cylinder submerged underwater in a constant velocity flow field directed along the undisturbed axis of the cylinder (Figure 1(a) and 1(b)). The upstream end of the cylinder is at $x = 0$ and the downstream end at $x = L$ and its small transverse (y direction) displacement is $v(x, t)$. The cylinder motion is therefore restricted to the xy plane. The angle ϕ (Figure 1(c)), which is the instantaneous angle made by the tangent to the cylinder axis at a point with the x-axis (or U vector), is assumed small and so is $\partial\phi/\partial x$, so that no cross-flow separation takes place. The physical boundaries of the fluid domain are assumed to be sufficiently away from the cylinder so that they do not influence the problem.

The momentum (in the y direction) associated with the velocity v is $M(\mathrm{D}v/\mathrm{D}t)$ per unit length of the cylinder and the rate of change of this momentum results in an equal and opposite (i.e., in $-y$ direction) inertial force F_A on the cylinder [12]

$$F_A = \frac{\mathrm{D}}{\mathrm{D}t}\left(M\frac{\mathrm{D}v}{\mathrm{D}t}\right) = M\left(\frac{\partial}{\partial t} + U\frac{\partial}{\partial x}\right)^2 v, \qquad \left[M = \varrho A = \frac{\pi D^2 \varrho}{4}; \frac{\mathrm{D}v}{\mathrm{D}t} = \frac{\partial v}{\partial t} + U\frac{\partial v}{\partial x}\right], \quad (1)$$

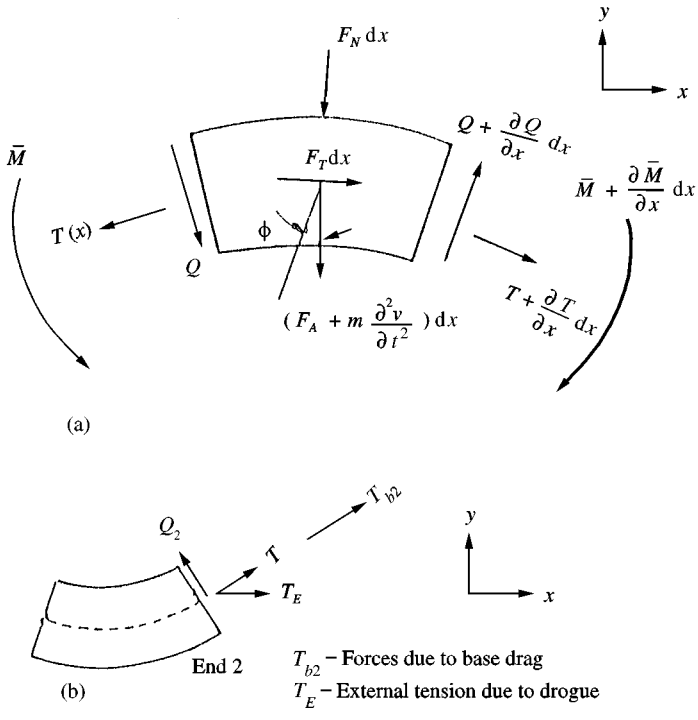

Figure 2. Forces and moments on an element of the cylinder: (a) interior element; (b) element at the downstream end.

where Dv/Dt is the resultant relative velocity between the cylinder and the fluid. The viscous forces are given by [13]

$$F_N = \frac{1}{2}\varrho U^2 D(C_D \sin^2\phi + C_N \sin\phi), \qquad F_T = \frac{1}{2}\varrho U^2 D C_T \cos\phi,$$

$$\phi = \phi(x,t) = \sin^{-1}\left(\frac{1}{U}\frac{Dv}{Dt}\right). \tag{2}$$

Since $\phi \ll 1$, F_N and F_T expressions can be linearized by setting $\sin^2\phi = 0$, $\sin\phi = \phi$ and $\cos\phi = 1$. In all numerical calculations in the literature, it is almost always assumed that

$$C_T = C_N = C_f \tag{3}$$

Linearization of equation (2) yields

$$F_N = \frac{1}{2}\varrho U D C_N\left(\frac{\partial v}{\partial t} + U\frac{\partial v}{\partial x}\right), \qquad F_T = \frac{1}{2}\varrho U^2 D C_T. \tag{4a}$$

Alternatively,

$$F_N = \frac{1}{2}c_N\frac{MU}{D}\left(\frac{\partial v}{\partial t} + U\frac{\partial v}{\partial x}\right), \qquad F_T = \frac{1}{2}c_T\frac{MU^2}{D}. \tag{4b}$$

Now consider an element of the cylinder of length dx (see Figure 2(a)), on which in addition to Q and $\bar{M}$, the other forces are (i) axial tension $T(x)$ directed along elastic line of the

cylinder, (ii) the transverse viscous force $F_N\,\mathrm{d}x$, (iii) the tangential viscous force $F_T\,\mathrm{d}x$, (iv) the transverse fluid inertial force $F_A\,\mathrm{d}x$ and (v) the transverse structure inertial force $m(\partial^2 v/\partial t^2)\,\mathrm{d}x$. The x-equilibrium (to the first order) is $\partial T/\partial x + F_T = 0$, which on integration between x to L results in

$$T(x) = T(L) + \tfrac{1}{2}\varrho U^2 DC_f(L - x). \tag{5}$$

For the case when both the ends are supported, let the initial tension be T_0, which involves an axial movement of the downstream support. Once the flow sets in, the support movement is not allowed so that the overall extension of the cylinder is zero under the frictional forces of the fluid. This requires $T(0) + T(L) = 2T_0$ which when used in equation (5), gives

$$T(L) = T_0 - \frac{1}{2}\varrho U^2 DC_f\left(\frac{L}{2}\right) \tag{6}$$

and in view of the above, equation (5) becomes

$$T(x) = T_0 + \frac{1}{2}\varrho U^2 DC_f\left(\frac{L}{2} - x\right). \tag{7}$$

For the case when the downstream end is free, the end tension $T(L)$ can be due to T_{b2} and T_E. The latter can be imposed in practice by a drogue (Figure 2(b)). Thus

$$T(L) = T_{b2} + T_E. \tag{8}$$

The base drag is usually taken to be proportional to $\rho U^2 A$ with appropriate base drag coefficients for upstream and downstream ends:

$$T_{bj} = \tfrac{1}{2} C_{bj}\varrho U^2 D^2, \quad j = 1, 2. \tag{9}$$

Both these base drags are directed along the instantaneous axis of the cylinder. However, T_E (say imposed by a drogue), may be considered as a constant directional force, the direction being parallel to U (or x-axis). The tension equations (5) and (7) can be combined as

$$T(x) = \frac{1}{2}\varrho U^2 DC_f\left[\left(1 - \frac{\gamma}{2}L\right) - x\right] + (1 - \gamma)T(L) + T_0\gamma. \tag{10}$$

The transverse equilibrium of the element in Figure 2(a) yields

$$\frac{\partial Q}{\partial x} - F_N - F_A + F_T\frac{\partial v}{\partial x} - m\frac{\partial^2 v}{\partial t^2} + \frac{\partial}{\partial x}\left(T\frac{\partial v}{\partial x}\right) = 0. \tag{11}$$

The moment equilibrium is $Q = \partial\bar{M}/\partial x$ which, in view of moment–curvature relation $\bar{M} = -EI\partial^2 v/\partial x^2$ results in

$$Q = -EI\frac{\partial^3 v}{\partial x^3}. \tag{12}$$

The last term of equation (11) may be written, in view of equations (4) and (10), as

$$\frac{\partial}{\partial x}\left(T\frac{\partial v}{\partial x}\right) = -\frac{1}{2}\varrho U^2 DC_f\frac{\partial v}{\partial x} + T\frac{\partial^2 v}{\partial x^2} = -F_T\frac{\partial v}{\partial x} + T\frac{\partial^2 v}{\partial x^2}. \tag{13}$$

Now in view of equations (1), (4), (10) and (13), equation (11) yields the governing differential equation [3]

$$EI\frac{\partial^4 v}{\partial x^4} + (m+M)\frac{\partial^2 v}{\partial t^2} + MU^2\frac{\partial^2 v}{\partial x^2} + 2MU\frac{\partial^2 v}{\partial x \partial t} - T\frac{\partial^2 v}{\partial x^2} + \frac{1}{2}\varrho DU\, C_f\left(\frac{\partial v}{\partial t} + U\frac{\partial v}{\partial x}\right) = 0. \tag{14}$$

The possible boundary conditions associated with this equation at the upstream and downstream ends of the cylinder are (i) simply supported (or pinned), (ii) clamped (or fixed), (iii) free and (iv) towed end (i.e., a free end attached to a tow rope). For the latter two conditions, the end shape is assumed to be either blunt or tapered. In case of a tapered end (up or downstream), the taper is assumed over a small length ($l_1, l_2 \ll L$, see Figures 1(a) and 1(b)) so that one can define

$$\chi_{e1} = \frac{1}{A}\int_0^{l_1} A(x)\,\mathrm{d}x, \qquad \chi_{e2} = \frac{1}{A}\int_{L-l_2}^{L} A(x)\,\mathrm{d}x. \tag{15}$$

The possible combination of boundary conditions at the two ends are (i) pinned–pinned, (ii) clamped–clamped (iii) pinned–clamped, (iv) clamped–pinned, (v) clamped–free, (vi) pinned–free, (vii) towed–free or (viii) free–free. The pinned and the clamped conditions are given by

$$v = \left.\frac{\partial^2 v}{\partial x^2}\right|_{x=0,L} = 0 \text{ (pinned) or } v = \left.\frac{\partial v}{\partial x}\right|_{x=0,L} = 0 \text{ (clamped).} \tag{16}$$

For a free end, however, the effect of taper at both ends must be accounted for since this significantly affects the dynamics and the stability of the cylinder. This has been proposed as [3]

$$\left[EI\frac{\partial^3 v}{\partial x^3} + f_1 MU\left(\frac{\partial v}{\partial t} + U\frac{\partial v}{\partial x}\right) + (m + f_1 M)\chi_{e1}\frac{\partial^2 v}{\partial t^2}\right]_{x=0} = 0, \tag{17a}$$

$$\left[EI\frac{\partial^3 v}{\partial x^3} + f_2 MU\left(\frac{\partial v}{\partial t} + U\frac{\partial v}{\partial x}\right) - (m + f_2 M)\chi_{e2}\frac{\partial^2 v}{\partial t^2}\right]_{x=L} = 0, \tag{17b}$$

where $f_i = 0$ for blunt and $f_i = 1$ for fully streamlined shapes. For a towed end, P enters into the boundary condition (see Figure 1), which equals the tension in the cylinder at the end $x = 0$ plus the form drag at this end (see equations (5), (8) and (9)):

$$P = T(0) + T_{b1}. \tag{18}$$

Following reference [3], the boundary condition at the towed end ($x = 0$) is given by

$$EI\frac{\partial^3 v}{\partial x^3} + f_1 MU\left(\frac{\partial v}{\partial t} + U\frac{\partial v}{\partial x}\right) + \frac{Pv}{s} + (m + f_1 M)\chi_{e1}\frac{\partial^2 v}{\partial t^2} = 0, \tag{19}$$

where the term Pv/s is the vertical component of the tow rope pull. The equation of motion (14) and the boundary conditions given by equations (16), (17) and (19) constitute the statement of the towed cylinder problem.

3. VARIATIONAL FORMULATION

Variational statement of a continuum mechanics problem is the most convenient and natural starting point in constructing its finite element approximation. In this section, Hamilton's principle will be used for this purpose. The Hamilton's principle may be written as

$$\int_{t_1}^{t_2} \delta(\bar{T} - \bar{V})\,\mathrm{d}t + \int_{t_1}^{t_2} \delta W_{nc}\,\mathrm{d}t = 0, \tag{20a}$$

$$\bar{T} = \bar{T}_1 + \bar{T}_2 + \bar{T}_3, \qquad \bar{V} = \bar{V}_1 + \bar{V}_2. \tag{20b}$$

The kinetic energy $\bar{T}_1$ is given by

$$\bar{T}_1 = \frac{1}{2}\int_0^L m\left(\frac{\partial v}{\partial t}\right)^2 \mathrm{d}x. \tag{21a}$$

The transverse component of the axial flow velocity U is $U(\partial v/\partial x)$ and therefore the total transverse velocity is $\partial v/\partial t + U\partial v/\partial x$ (see equation (1)). Therefore, the kinetic energy $\bar{T}_2$ is given by

$$\begin{aligned}\bar{T}_2 &= \frac{1}{2}M\int_0^L \left(\frac{\partial v}{\partial t} + U\frac{\partial v}{\partial x}\right)^2 \mathrm{d}x \\ &= \frac{1}{2}M\int_0^L \left(\frac{\partial v}{\partial t}\right)^2 \mathrm{d}x + \frac{1}{2}MU^2\int_0^L \left(\frac{\partial v}{\partial x}\right)^2 \mathrm{d}x + MU\int_0^L \frac{\partial v}{\partial t}\frac{\partial v}{\partial x}\,\mathrm{d}x \\ &= T_{2A} + T_{2B} + T_{2C}.\end{aligned} \tag{21b}$$

The taper at an end (up or downstream) which is assumed to be short can be visualized as a lumped structural mass without any rotatory inertia, as well as a lumped added mass. Thus, the kinetic energy $\bar{T}_3$ is given by

$$\bar{T}_3 = \sum_{i=1}^{2} \frac{1}{2}\bar{m}_i\left(\frac{\partial v_i}{\partial t}\right)^2. \tag{21c}$$

The expressions for $\bar{V}_1$ and $\bar{V}_2$ are given by

$$\bar{V}_1 = \frac{1}{2}EI\int_0^L \left(\frac{\partial^2 v}{\partial x^2}\right)^2 \mathrm{d}x, \qquad \bar{V}_2 = \frac{1}{2}\int_0^L T(x)\left(\frac{\partial v}{\partial x}\right)^2 \mathrm{d}x. \tag{22}$$

The work done by F_T and F_N during variation δv is given by

$$\delta W_{nc} = \int_0^L \left(F_T\frac{\partial v}{\partial x} - F_n\right)\delta v\,\mathrm{d}x. \tag{23}$$

In addition to the above, the terms representing (i) the effect of end shapes (up and downstream) on the system dynamics (ii) the effect of the tow rope pull at the upstream end, (iii) the effect of the base drags (up and downstream ends) and (iv) the effect of the drag due to drougue (downstream end) should also be included. However, instead of doing this formally in a rigorous manner, advantage is taken of the already known boundary conditions presented in reference [3] which are given by equations (17) and (19) and their variational forms are directly used in developing their finite element approximations. Thus,

Hamilton's principle for the present problem may be written as

$$\int_{t_1}^{t_2} (\delta \bar{T}_1 + \delta \bar{T}_2 - \delta \bar{V}_1 - \delta \bar{V}_2 + \delta W_{nc})\,\mathrm{d}t + \delta\left(\frac{1}{2}\int_{t_1}^{t_2} \bar{m}_1 \left(\frac{\partial v}{\partial t}\right)_0^2 \mathrm{d}t\right)$$

$$+ \delta\left(\frac{1}{2}\int_{t_1}^{t_2} \bar{m}_2 \left(\frac{\partial v}{\partial t}\right)_L^2 \mathrm{d}t\right) + \text{other boundary terms} = 0, \tag{24}$$

where the first end may be supported or towed or free, the second end may be supported or free with a drogue attached to it (see Figure 2(b)). A possible form of $\bar{m}_i$ as used in the literature (see equation (17)) is

$$\bar{m}_i = (m + f_i M)\,\chi_{ei} \quad (i = 1, 2). \tag{25}$$

The indicated variation of various terms and their integration appearing in equation (24) can now be carried out using "by-part" integration. These are recorded below term by term. The by-part integration operation with respect to t gives rise to two "end" terms, one each at times t_1 and t_2. These terms can be discarded by assuming suitable initial conditions. So, without loss of generality, such terms have been left out in the following expressions:

$$\int_{t_1}^{t_2} \delta \bar{T}_1\,\mathrm{d}t = \int_{t_1}^{t_2} \mathrm{d}t \left[\int_0^L m\left(\frac{\partial v}{\partial t}\right)\delta\left(\frac{\partial v}{\partial t}\right)\mathrm{d}x\right] = \int_{t_1}^{t_2} \mathrm{d}t\left[-\int_0^L m\frac{\partial^2 v}{\partial t^2}\,\delta v\,\mathrm{d}x\right],$$

$$\int_{t_1}^{t_2} \delta \bar{T}_2\,\mathrm{d}t = \int_{t_1}^{t_2} \mathrm{d}t \int_0^L \left[M\frac{\partial v}{\partial t}\,\delta\left(\frac{\partial v}{\partial t}\right) + MU^2\frac{\partial v}{\partial x}\delta\left(\frac{\partial v}{\partial x}\right) + MU\frac{\partial v}{\partial t}\delta\left(\frac{\partial v}{\partial x}\right)\right.$$

$$\left. + MU\frac{\partial v}{\partial x}\delta\left(\frac{\partial v}{\partial t}\right)\right]\mathrm{d}x = \int_{t_1}^{t_2} \mathrm{d}t \int_0^L \left[-M\frac{\partial^2 v}{\partial t^2} - MU^2\frac{\partial^2 v}{\partial x^2} - 2MU\frac{\partial^2 v}{\partial x \partial t}\right]\delta v\,\mathrm{d}x$$

$$+ \int_{t_1}^{t_2} \mathrm{d}t\left[MU^2\frac{\partial v}{\partial x}\,\delta v + MU\frac{\partial v}{\partial t}\,\delta v\right]_0^L,$$

$$\int_{t_1}^{t_2} \delta V_1\,\mathrm{d}t = \int_{t_1}^{t_2} \mathrm{d}t\left[\int_0^L EI\frac{\partial^2 v}{\partial x^2}\delta\left(\frac{\partial^2 v}{\partial x^2}\right)\mathrm{d}x\right] = \int_{t_1}^{t_2} \mathrm{d}t \int_0^L EI\frac{\partial^4 v}{\partial x^4}\delta v\,\mathrm{d}x$$

$$+ \int_{t_1}^{t_2} \mathrm{d}t\left[EI\frac{\partial^2 v}{\partial x^2}\,\delta\left(\frac{\partial v}{\partial x}\right) - EI\frac{\partial^3 v}{\partial x^3}\,\delta v\right]_0^L,$$

$$\int_{t_1}^{t_2} \delta V_2\,\mathrm{d}t = \int_{t_1}^{t_2} \mathrm{d}t\left[\int_0^L T\frac{\partial v}{\partial x}\,\delta\left(\frac{\partial v}{\partial x}\right)\mathrm{d}x\right] = \int_{t_1}^{t_2} \mathrm{d}t \int_0^L -\frac{\partial}{\partial x}\left(T\frac{\partial v}{\partial x}\right)\delta v\,\mathrm{d}x$$

$$+ \int_{t_1}^{t_2} \mathrm{d}t\left[T\frac{\partial v}{\partial x}\delta v\right]_0^L,$$

$$\int_{t_1}^{t_2} \delta\left(\frac{1}{2}\bar{m}_i\left(\frac{\partial v_i}{\partial t}\right)^2\right) = \int_{t_1}^{t_2} \mathrm{d}t\left(-\bar{m}_i\left(\frac{\partial^2 v_i}{\partial t^2}\right)\delta v\right). \tag{26}$$

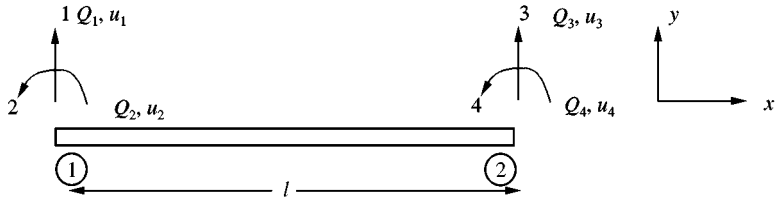

Figure 3. Two-dimensional beam element.

Using equations (26) in equation (24), one obtains

$$\int_{t_1}^{t_2} \mathrm{d}t \int_0^L \left[-(m+M)\frac{\partial^2 v}{\partial t^2} - MU^2 \frac{\partial^2 v}{\partial x^2} - 2MU \frac{\partial^2 v}{\partial x \partial t} - EI \frac{\partial^4 v}{\partial x^4} + \frac{\partial}{\partial x}\left(T(x) \frac{\partial v}{\partial x} \right) + F_T \frac{\partial v}{\partial x} - F_N \right] \delta v \, \mathrm{d}x + \text{boundary terms} = 0. \tag{27}$$

The variation δv being arbitrary, the expression in the square bracket in equation (27) yields the equation of motion:

$$EI \frac{\partial^4 v}{\partial x^4} + (m+M)\frac{\partial^2 v}{\partial t^2} + MU^2 \frac{\partial^2 v}{\partial x^2} + 2MU \frac{\partial^2 v}{\partial x \partial t} - \frac{\partial}{\partial x}\left(T(x) \frac{\partial v}{\partial x} \right) - F_T \frac{\partial v}{\partial x} + F_N = 0. \tag{28}$$

It can be readily verified that equation (28) is identical to equation (14) in view of equations (4) and (13). The boundary conditions are given by equations (16), (17) and (19).

4. FINITE ELEMENT APPROXIMATION

The finite element approximation of the problem will be developed here from Hamilton's principle. The finite element chosen is a two-noded straight uniform two-dimensional beam element with two bending degrees of freedom in the xy plane at each node. The beam element of length l is shown in Figure 3 and its displacement field is given by [14]

$$v(\bar{x}, t) = \sum_{i=1}^{4} N_i(\bar{x}) u_i(t),$$

$$N_1 = 1 - 3\bar{s}^2 + 2\bar{s}^3, \qquad N_2 = (\bar{s} - 2\bar{s}^2 + \bar{s}^3) l, \qquad N_3 = 3\bar{s}^2 - 2\bar{s}^3,$$

$$N_4 = (-\bar{s}^2 + \bar{s}^3) l, \tag{29}$$

where $\bar{s} = \bar{x}/l$. The various terms appearing in Hamilton's principle given by equation (24) will be treated below with appropriate substitutions from equation (29). However, since several terms result in well known standard matrices of this elementary beam element, these are not treated in detail. Substituting equation (21a) in equation (24) and using equation

(29), the integral involving $\bar{T}_1$ gives

$$\int_{t_1}^{t_2} \delta \bar{T}_1 \, dt = -\int_{t_1}^{t_2} dt \left[m \int_0^l N_i N_j \, dx \, \ddot{u}_j \delta u_i \right];$$

$$\int_{t_1}^{t_2} \delta T_{2A} \, dt = -\int_{t_2}^{t_1} dt \left[\left(M \int_0^l N_i N_j \, dx \right) \ddot{u}_j \delta u_i \right]. \tag{30a}$$

Substituting first of equation (22) into equation (24) and using equation (29), the integral involving $\bar{V}_1$ gives

$$\int_{t_1}^{t_2} \delta \bar{V}_1 \, dt = \int_{t_1}^{t_2} dt \left[\left(EI \int_0^l N_i'' N_j'' \, dx \right) u_j \delta u_i \right]. \tag{30b}$$

The integrals involving T_{2B} and $\bar{V}_2$ are similar. Similar operation on the former using equation 21(b) gives

$$\int_{t_1}^{t_2} \delta T_{2B} \, dt = \int_{t_1}^{t_2} dt \left[MU^2 \int_0^l \frac{\partial v}{\partial x} \delta \left(\frac{\partial v}{\partial x} \right) dx \right] = \int_{t_1}^{t_2} dt \left[\left(MU^2 \int_0^l N_i' N_j' \, dx \right) u_j \delta u_i \right]. \tag{30c}$$

Similarly, using second of equation (22) gives

$$\int_{t_1}^{t_2} \delta \bar{V}_2 \, dt = \int_{t_1}^{t_2} dt \left[\left(\int_0^l T(x) N_i' N_j' \, dx \right) u_j \delta u_i \right]. \tag{30d}$$

Substituting equation (21b) into equation (24) and using equation (29), the integral involving T_{2C} gives

$$\begin{aligned} \int_{t_2}^{t_1} \delta T_{2C} \, dt &= \int_{t_2}^{t_1} dt \left[MU \int_0^l \frac{\partial}{\partial t} (\delta v) \frac{\partial v}{\partial x} \, dx + MU \int_0^l \frac{\partial v}{\partial t} \frac{\partial}{\partial x} (\delta v) \, dx \right] \\ &= -\int_{t_1}^{t_2} dt \left[MU \int_0^l \frac{\partial}{\partial x} \left(\frac{\partial v}{\partial t} \right) \delta v \, dx \right] + \int_{t_1}^{t_2} dt \left[MU \int_0^l \frac{\partial v}{\partial t} \frac{\partial}{\partial x} (\delta v) \, dx \right] \\ &= \int_{t_1}^{t_2} dt \left[\left(MU \int_0^l (N_j N_i' - N_j' N_i) \right) \dot{u}_j \delta u_i \right]. \end{aligned} \tag{30e}$$

In all the above equations where indices i and j are repeated, double-summation convention is implied. Consider now the term involving W_{nc} in equation (23). In view of equation (4), the terms involving F_T and F_N may be written as

$$F_T \frac{\partial v}{\partial x} - F_N = \alpha_1 \frac{\partial v}{\partial x} - \alpha_2 \frac{\partial v}{\partial t}, \qquad \alpha_1 = \frac{1}{2} \frac{MU^2}{D} (c_T - c_N), \qquad \alpha_2 = \frac{1}{2} c_N \frac{MU}{D}. \tag{30f}$$

In view of the above, the integral in equation (23), on using equation (29) may be written as

$$\begin{aligned} \int_{t_1}^{t_2} \delta W_{nc} \, dt &= \int_{t_1}^{t_2} dt \left[\alpha_1 \int_0^l \frac{\partial v}{\partial x} \delta v \, dx - \alpha_2 \int_0^l \frac{\partial v}{\partial t} \delta v \, dx \right] \\ &= \int_{t_1}^{t_2} dt \left[\left(\alpha_1 \int_0^1 N_j' N_i \, dx \right) u_j \delta u_i \right] - \int_{t_1}^{t_2} dt \left[\left(\alpha_2 \int_0^l N_i N_j \, dx \right) \dot{u}_j \delta u_i \right]. \end{aligned} \tag{30g}$$

Using equation (29) in the second integral in equation (24), which is defined at the end $x = 0$, yields

$$\delta \int_{t_1}^{t_2} \frac{1}{2} \bar{m}_1 \left(\frac{\partial v}{\partial t}\right)_0^2 \mathrm{d}t = \bar{m}_1 \left(\frac{\partial v}{\partial t}\right)_0 \delta v_0 \Big|_{t_1}^{t_2} - \bar{m}_1 \int_{t_1}^{t_2} \left(\frac{\partial^2 v}{\partial t^2}\right)_0 \delta v_0 \, \mathrm{d}t$$

$$= \int_{t_1}^{t_2} \mathrm{d}t[(-\bar{m}_1 N_i(0) N_j(0)) \ddot{u}_j \delta u_i], \tag{30h}$$

where the first term in the second step above drops out due to initial conditions. Similarly, the third integral in equation (24), defined at the end $x = l$ gives

$$\delta \int_{t_1}^{t_2} \frac{1}{2} \bar{m}_2 \left(\frac{\partial v}{\partial t}\right)_1^2 \mathrm{d}t = \int_{t_1}^{t_2} \mathrm{d}t \, [(-\bar{m}_2 N_i(l) N_j(l)) \ddot{u}_j \delta u_i], \tag{30i}$$

where the suffix l indicates location $x = l$.

The boundary terms that contribute to equation (24) can be inferred from the boundary conditions (17a,b) and (19). The contributions of the fluid dynamic terms and the component of the tow rope pull will be developed now. At the end $x = 0$, using equation (29), we get from equation (17a) or (19)

$$\int_{t_1}^{t_2} \bar{f}_1 MU \left(\left(\frac{\partial v}{\partial t}\right)_0 + U \left(\frac{\partial v}{\partial x}\right)_0 \right) \delta v \, \mathrm{d}t$$

$$= \int_{t_1}^{t_2} \mathrm{d}t \, [(\bar{f}_1 MU \, N_i(0) N_j(0)) \dot{u}_j \delta u_i] + \int_{t_1}^{t_2} [(\bar{f}_1 MU^2 N_j'(0) N_i(0)) u_j \delta u_i]. \tag{30j}$$

Similarly, at the end $x = l$, we get from equation (17b),

$$\int_{t_1}^{t_2} \bar{f}_2 MU \left(\left(\frac{\partial v}{\partial t}\right)_l + U \left(\frac{\partial v}{\partial x}\right)_l \right) \delta v \, \mathrm{d}t$$

$$= \int_{t_1}^{t_2} \mathrm{d}t \, [(\bar{f}_2 MU \, N_i(l) N_j(l)) \dot{u}_j \delta u_i] + \int_{t_1}^{t_2} [(\bar{f}_2 MU^2 N_j'(l) N_i(l)) u_j \delta u_i]. \tag{30k}$$

The contribution of the term involving two rope pull P in equation (19) can be written as

$$\int_{t_1}^{t_2} \frac{P v_0}{s} \delta v \, \mathrm{d}t = \int_{t_1}^{t_2} \mathrm{d}t \left[\left(\frac{P}{s} N_j(0) N_i(0) \right) u_j \delta u_i \right], \tag{30l}$$

where the suffix 0 indicates location $x = 0$. Substituting equations (30) into equation (24) and rearranging and noting that δu_i is arbitrary, one obtains the element equations of motion, which can be assembled by standrad procedures. Thus, the global equations of motion may be written as

$$[m]\{\ddot{u}\} + [c]\{\dot{u}\} + [k]\{u\} = \{0\}; \left[[m] = \sum_{el} [m^e], [c] = \sum_{el} [c^e], [k] = \sum_{el} [k^e] \right], \tag{31}$$

where $\{u\}$ is the vector of all degrees of freedom in the structure and $\sum_{el}$ denotes finite element assemblage operation over all elements. The element mass, damping and stiffness

matrices $[m^e]$, $[c^e]$ and $[k^e]$ are given by

$$m_{ij}^e = \bar{m}_{ij} + \hat{m}_{ij}^{(1)} + \hat{m}_{ij}^{(2)}, \qquad c_{ij}^e = \bar{c}_{ij} + \hat{c}_{ij}^{(1)} + \hat{c}_{ij}^{(2)}, \qquad k_{ij}^e = \bar{k}_{ij} + \hat{k}_{ij}^{(1)} + \hat{k}_{ij}^{(2)} + \hat{k}_{ij}^{(p)}. \quad (32)$$

The various matrices above are

$$\bar{m}_{ij} = \bar{m}_{ij}^{(1)} + \bar{m}_{ij}^{(2)} = m \int_0^l N_i N_j \, \mathrm{d}x + M \int_0^l N_i N_j \, \mathrm{d}x,$$

$$\bar{c}_{ij} = \bar{c}_{ij}^{(1)} + \bar{c}_{ij}^{(2)} = \frac{1}{2} c_N \frac{MU}{D} \int_0^l N_i N_j \, \mathrm{d}x - MU \int_0^l (N_j N_i' - N_j' N_i) \, \mathrm{d}x,$$

$$\bar{k}_{ij} = \bar{k}_{ij}^{(1)} + \bar{k}_{ij}^{(2)} + \bar{k}_{ij}^{(3)} + \bar{k}_{ij}^{(4)} = EI \int_0^l N_i'' N_j'' \, \mathrm{d}x$$

$$+ \int_0^l T(x) N_i' N_j' \, \mathrm{d}x - MU^2 \int_0^l N_i' N_j' \, \mathrm{d}x,$$

$$- \frac{1}{2} \frac{MU^2}{D} (c_N - c_T) \int_0^l N_j' N_i \, \mathrm{d}x,$$

$$\hat{m}_{ij}^{(1)} = (m + f_1 M) \chi_{e1} N_i(0) N_j(0), \qquad \hat{m}_{ij}^{(2)} = (m + f_2 M) \chi_{e2} N_i(l) N_j(l),$$

$$\hat{c}_{ij}^{(1)} = \bar{f}_1 MU N_i(0) N_j(0), \qquad \hat{c}_{ij}^{(2)} = -\bar{f}_2 MU N_i(l) N_j(l),$$

$$\hat{k}_{ij}^{(1)} = \bar{f}_1 MU^2 N_j'(0) N_i(0), \qquad \hat{k}_{ij}^{(2)} = -\bar{f}_2 MU^2 N_j'(l) N_i(l),$$

$$\hat{k}_{ij}^{(p)} = \frac{P}{s} N_i(0) N_j(0). \quad (33)$$

It should be noted that the matrices $\hat{m}_{ij}^{(1)}$, $\hat{c}_{ij}^{(1)}$, $\hat{k}_{ij}^{(1)}$ and $\hat{k}_{ij}^{(p)}$ are non-trivial only for the element whose $x = 0$ end is the upstream end of the structure. Similarly the matrices $\hat{m}_{ij}^{(2)}$, $\hat{c}_{ij}^{(2)}$ and $\hat{k}_{ij}^{(2)}$ are non-trivial only for the element whose $x = l$ end is the downstream (free) end of the structure. The various matrices are: $\bar{m}_{ij}^{(1)}$ is the structural mass matrix, $\bar{m}_{ij}^{(2)}$ is the added mass matrix, $\bar{c}_{ij}^{(1)}$ is the viscous fluid damping matrix, $\bar{c}_{ij}^{(2)}$ is the inviscid fluid damping matrix, $\bar{k}_{ij}^{(1)}$ is the elastic stiffness matrix, $\bar{k}_{ij}^{(2)}$ is the geometric stiffness matrix, $\bar{k}_{ij}^{(3)}$ is the inviscid fluid stiffness matrix and $\bar{k}_{ij}^{(4)}$ is the viscous fluid stiffness matrix. The various shape-function-related parts of these matrices which are not common are given below:

$$\left[\int_0^l (N_j N_i' - N_j' N_i) \, \mathrm{d}x \right] = \begin{bmatrix} 0 & \frac{l}{5} & 1 & -\frac{l}{5} \\ -\frac{l}{5} & 0 & \frac{l}{5} & -\frac{l^2}{30} \\ -1 & -\frac{l}{5} & 0 & \frac{l}{5} \\ \frac{l}{5} & \frac{l^2}{30} & -\frac{l}{5} & 0 \end{bmatrix},$$

$$\left[\int_0^l N_j' N_i \, \mathrm{d}x\right] = \begin{bmatrix} -\frac{1}{2} & \frac{l}{10} & \frac{1}{2} & -\frac{l}{10} \\ -\frac{l}{10} & 0 & \frac{l}{10} & -\frac{l^2}{60} \\ -\frac{1}{2} & -\frac{l}{10} & \frac{1}{2} & \frac{l}{10} \\ \frac{l}{10} & \frac{l^2}{60} & -\frac{l}{10} & 0 \end{bmatrix},$$

$$[N_i(0)\, N_j(0)] = \begin{bmatrix} 1 & 0 & 0 & 0 \\ 0 & 0 & 0 & 0 \\ 0 & 0 & 0 & 0 \\ 0 & 0 & 0 & 0 \end{bmatrix}, \qquad [N_j'(0)\, N_i(0)] = \begin{bmatrix} 0 & 0 & 0 & 0 \\ 1 & 0 & 0 & 0 \\ 0 & 0 & 0 & 0 \\ 0 & 0 & 0 & 0 \end{bmatrix},$$

$$[N_i(l)\, N_j(l)] = \begin{bmatrix} 0 & 0 & 0 & 0 \\ 0 & 0 & 0 & 0 \\ 0 & 0 & 1 & 0 \\ 0 & 0 & 0 & 0 \end{bmatrix}, \qquad [N_j'(l)\, N_i(l)] = \begin{bmatrix} 0 & 0 & 0 & 0 \\ 0 & 0 & 0 & 0 \\ 0 & 0 & 0 & 1 \\ 0 & 0 & 0 & 0 \end{bmatrix}. \tag{34}$$

In view of equation (34), it may be seen that $\bar{c}_{ij}^{(2)}$ is a skew symmetric matrix and $\bar{k}_{ij}^{(4)}$ is an unsymmetric with $\bar{k}_{ij}^{(4)} = -\bar{k}_{ij}^{(4)}$ for $i \neq j$. Carrying out harmonic decomposition (i.e., $u_j = u_{j0} \exp(\mathrm{i}\omega t)$) of the finite element equations of motion given by equation (31), one obtains the following quadratic eigenproblem:

$$[-\omega^2 [m] + \mathrm{i}\omega [c] + [k]]\{u\} = 0. \tag{35}$$

The eigenvalues are obtained as the roots of the determinantal equation

$$\det[-\omega^2 [m] + \mathrm{i}\omega [c] + [k]] = 0. \tag{36}$$

The roots ω are complex with the property that if ω is a root, then $-\omega^*$ is also a root (a* denoting complex conjugate). The real part of ω represents the frequency of oscillation and the imaginary part of ω represents the damping induced by fluid flow. Thus, a positive $\mathrm{Im}(\omega)$ indicates damped motion and hence a stable system, whereas a negative $\mathrm{Im}(\omega)$ indicates instability.

5. COMPUTER IMPLEMENTATION

The subroutine tree of the development FE code is shown in Figure 4. The description of the functions of the various subroutines is given below in brief.

1. S1 reads the degrees of freedom (d.o.f.) and co-ordinates of the nodes and also assigns equation numbers to these degrees of freedom.
2. S2 reads data sets of material, sectional and hydrodynamic properties of all elements used. Then it reads element connectivity data in an element loop and calls S3–S10 to calculate various element matrices. It also calls S11 for transformation of these element matrices and S12 to calculate end tensions based on a formula, if any. In the absence of

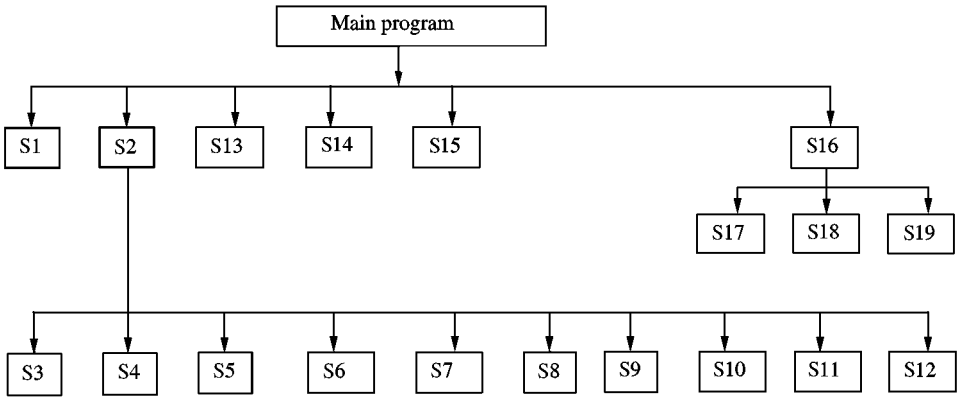

Figure 4. Subroutine tree of finite element code.

any such formula, the values of the end tensions of an element are read along with element data. These values are then user supplied. The point matrices for the free and elements are also calculated in this routine. It then sums up all the matrices appropriately (i.e., stiffness, mass and damping matrices) and writes them on a scratch unit.

3. S3 calculates the elastic stiffness matrix, S4 the geometric stiffness matrix for linearly varying axial load, S5 the inviscid fluid stiffness matrix, S6 the viscous fluid stiffness matrix, S7 the inviscid fluid damping matrix, S8 the viscous fluid damping matrix, S9 the structural mass matrix and S10 the added mass matrix.
4. S11 transforms an element matrix in element co-ordinate system to global co-ordinate system.
5. S12 implements a user-selected formula to calculate tension at a node (point) based on its coordinates.
6. S13 reads the nodal masses, if any.
7. S14 adds the nodal masses to the global mass matrix.
8. S15 is the assembly routine.
9. S16 is the controlling routine for the task of eigenvalue extraction by determinant search using Newton–Raphson iteration scheme. The iteration loop is set up in this routine which calls S17 for complex determinant evaluation and S18 for Newton–Raphson iteration for complex roots.
10. S19 calculates eigenvector for a successfully computed complex eigenvalue.

The program is fairly compact consisting of about 1000 FORTRAN statements and has been written with the aim of achieving least computational time as well as sufficiently general memory management scheme. A tolerance of 1E–05 on roots gives good accuracy and requires about 10–15 iterations to converge for most cases. For relatively large determinants, a determinant scaling technique was required to avoid overflow and this was implemented in the code. All calculations were done is double precision.

6. VALIDATION AND CONVERGENCE STUDIES

First three validation problems, which are worked out using the FE code developed, have been chosen from the literature. These are concerned with one clamped–free [15] and two

towed–free [3] boundary conditions. For the purpose of validation, the finite element results are compared with those obtained from the analytical method of solution, namely the power series method, which also have been coded. The details of this method are available is reference [6] for pinned–pinned and clamped–clamped boundary conditions. For completeness, the extension to clamped–free and towed–free boundary conditions has been provided in Appendix A, which closely follows and complements the treatment in reference [6]. Original references may be consulted for more details of these example problems. Comparison of complex frequencies for a few flow velocities in each case are presented in Table 1. The convergence of the finite element method is brought out in Table 2 for two of these problems. These and other results are given in non-dimensional form.

In the case if rigid towed–free cylinder, which is a limiting case of an elastic one, two lowest modes with frequencies $\omega_0 = \omega_1 = 0$ at $u = 0$ are referred to as the zeroth and first modes, respectively, and at very low speeds these are associated with rigid body motion. The zeroth mode does not have a real part and the instability due to this mode is referred to as "yawing motion". The comparison for this case is given in Table 3.

As can be seen from Tables 1 and 3, the comparison between the analytical and the finite element results are as good as they could probably be, leaving very little to discuss. The convergence results in Table 2 and more of similar studies for many cases which were carried out, yield the following conclusions:

(a) For lower flow velocities, 10 elements are required for accurate results.
(b) For higher flow velocities and for higher modes of practical interest, 16 elements are required.
(c) A 2–4-element model gives reasonably good results for the first two modes.

To sum up, a 4-element model can be used for the first two roots, a 10-element model for all roots at lower flow velocities and a 16-element model for all situations that could be of practical interest.

The finite element model can also be used for string, i.e., cylinders with zero bending rigidity for which the earlier analytical theory (for finite to infinite bending rigidity) fails. In this connection, the work of reference [4] on strings in axial flow is of interest. In this work it was proved (without numerical result) that a neutrally buoyant pinned–free string is stable under any one of the two conditions which are: (i) the external tension at the free and exceeds the value of MU^2 or (ii) the slenderness ratio (ε) exceeds the value of $\pi/(2C_f)$.

To validate these conditions numerically, an example has been chosen and the results for this case are presented in Table 4 wherein three values of εc_f (namely 1, 1·5 and 0·5) and two different flow velocities (namely 1 and 3 m/s) were considered. The dimensional complex eigenfrequencies of the lowest two modes for both tapered and blunt ends are presented. It can be observed that for a value of $\varepsilon c_f = 1$, the roots are negative indicating that string is unstable for both streamlined as well as blunt ends, but when an external tension ($T_0 = MU^2 = 2{\cdot}01$ and 18·13 N for $U = 1$ and 3 m/s respectively) is applied, the roots are positive and hence the string is stable and satisfies one of the conditions. At a higher value of $\varepsilon c_f = 1{\cdot}5$ and at $U = 3$ m/s, the string is again unstable and an external tension $T_0 = MU^2$ has been applied to regain the stability of the string. On the other hand, for a value of $\varepsilon c_f = 2{\cdot}05$, the string remains quite stable for a blunt end for both the flow velocities and there is no necessity for any external tension to make it stable. This satisfies the second condition. Therefore, these results bear out the validity of these conditions appropriately and also demonstrate the capability of the FEM to treat the string in axial flow problems.

TABLE 1

Comparison of frequencies from analytical and finite element methods for various flow velocities

u	Ω (Analytical)	Ω (Finite element)
(a) *Clamped–free cylinder*: $\beta = 0{\cdot}5$, $\varepsilon c_f = 1$, $f_2 = 0{\cdot}8$, $c_{b2} = 0$, $\bar{\chi}_{e2} = 0{\cdot}01$		
0	3·4543 + i0·0	3·4543 + i0·0
	21·6592 + i0·0	21·6592 + i0·0
	60·6737 + i0·0	60·6758 + i0·0
2	0·0 + i1·5620	0·0 + i1·5620
	0·0 + i0·3000	0·0 + i0·3001
	20·3157 + i0·8408	20·3158 + i0·8408
	59·3765 + i0·8224	59·3788 + i0·8222
4	0·0 − i2·6115	0·0 − i2·6115
	0·0 + i7·2446	0·0 + i7·2446
	15·8984 + i1·4120	15·8986 + i1·4120
	55·3831 + i1·5744	55·3863 + i1·5746
(b) *Towed–free cylinder*: $\beta = 0{\cdot}5$, $\Lambda = 1$, $\varepsilon c_N = \varepsilon c_T = 1$, $f_1 = f_2 = 1$, $c_{b1} = c_{b2} = 0$, $\bar{\chi}_{e1} = \bar{\chi}_{e2} = 0{\cdot}01$		
1	0·0 − i1·7934	0·0 − i1·7934
	0·0 + i2·5089	0·0 + i2·5089
	0·9496 + i0·0035	0·9496 + i0·0035
	20·8952 + i0·1556	20·8952 + i0·1556
	58·9768 + i0·1604	58·9787 + i0·1604
3	0·0 − i3·8169	0·0 − i3·8063
	0·0 + i6·8490	0·0 + i6·8499
	2·9147 + i0·5276	2·9147 + i0·5276
	14·4695 − i0·1619	14·4696 − i0·1619
	55·0706 + i0·3531	55·0730 + i0·3531
6	5·6156 − i0·2184	5·6156 − i0·2185
	4·6183 − i13·0935	4·6186 − i13·0949
	39·5282 − i1·3510	39·5322 − i1·3509
(c) *Towed–free cylinder*: $\beta = 0{\cdot}5$, $\Lambda = 1$, $\varepsilon c_N = \varepsilon c_T = 1$, $f_1 = f_2 = 0{\cdot}7$, $c_{b1} = 0$, $c_{b2} = 0{\cdot}3$, $\bar{\chi}_{e1} = \bar{\chi}_{e2} = 0{\cdot}01$		
1	0·0 + i1·9071	0·0 + i1·9071
	1·3502 − i0·1449	1·3502 − i0·1449
	21·2766 + i0·1574	21·2767 + i0·1574
	59·4644 + i0·1623	59·4664 + i0·1623
3	0·0 + i4·9562	0·0 + i4·9562
	0·0 − i1·7075	0·0 − i1·7075
	4·1357 + i0·1129	4·1357 + i0·1129
	17·9166 + i0·1109	17·9167 + i0·1109
	57·1038 + i0·3810	57·1064 + i0·3810
6	5·8443 − i1·3503	5·8443 − i1·3503
	5·2949 + i13·5007	5·2950 + i13·5008
	48·3901 − i0·3799	48·3946 − i0·3798[a]

Note: Number of elements used are between 10 and 16.

TABLE 2

Convergence study of finite element solution

Method	Ω	
(a) *Clamped–free cylinder*: $\beta = 0{\cdot}5$, $\varepsilon c_f = 1$, $f_2 = 0{\cdot}8$, $c_{b2} = 0$, $\bar{\chi}_{e2} = 0{\cdot}01$		
	$u = 1$	$u = 3$
ANL	2·9513 + i0·4491	0·0 − i2·1421
	21·3269 + i0·4269	18·5673 + i1·2084
	60·3508 + i0·4143	57·7325 + i1·2143
FE(2)	2·9533 + i0·4497	0·0 − i2·1442
	21·5309 + i0·4317	18·9947 + i1·2424
	73·3809 + i0·4733	71·6192 + i1·3967
FE(4)	2·9515 + i0·4491	0·01 − i1·4212
	21·3522 + i0·4280	19·5290 + i1·2297
	60·8095 + i0·4198	59·2159 + i1·2341
FE(8)	2·9513 + i0·4491	0·0 − i2·1421
	21·3286 + i0·4270	18·5700 + i1·2087
	60·3864 + i0·4148	57·7765 + i1·2160
FE(16)	2·9513 + i0·4491	0·0 − i2·1421
	21·3270 + i0·4269	18·5675 + i1·2084
	60·3531 + i0·4144	57·7354 + i1·2144
(b) *Towed–free cylinder*: $\beta = 0{\cdot}5$, $\Lambda = 1$, $\varepsilon c_N = \varepsilon c_T = 1$, $f_1 = f_2 = 1$, $c_{b1} = c_{b2} = 0$ $\bar{\chi}_{e1} = \bar{\chi}_{e2} = 0{\cdot}01$		
	$u = 2$	$u = 4$
ANL	0·0 − i3·2819	2·5740 − i0·9693
	0·0 + i4·8984	8·5926 − i5·2939
	1·9188 + i0·0703	51·4341 + i0·2627
	18·7973 + i0·2348	
	57·5404 + i0·2923	
FE(2)	0·0 − i3·2821	2·4905 − i0·9648
	0·0 + i4·9012	9·0262 − i5·1416
	1·9188 + i0·0698	60·6192 + i0·2565
	18·9903 + i0·2455	
	65·7997 + i0·2897	
FE(4)	0·0 − i3·2819	2·5685 − i0·9691
	0·0 + i4·8986	8·6234 − i5·2885
	1·9188 + i0·0702	51·9877 + i0·2727
	18·8246 + i0·2353	
	57·9238 + i0·2933	
FE(8)	0·0 − i3·2817	2·5736 − i0·9693
	0·0 + i4·8985	8·5946 − i5·2936
	1·9188 + i0·0702	51·4789 + i0·2632
	18·7992 + i0·2342	
	57·5742 + i0·2923	
FE(16)	0·0 − i3·2819	2·5739 − i0·9693
	0·0 + i4·8984	8·5927 − i5·2939
	1·9188 + i0·0703	51·4369 + i0·2627
	18·7973 + i0·2348	
	57·5425 + i0·2923	

TABLE 3

Rigid body mode and flexible mode frequencies by analtyical and FEM: $\beta = 0.5$, $\varepsilon c_N = \varepsilon c_T = 1, f_1 = 1$, $c_{b1} = 0$, $c_{b2} = 1 - f_2$, $\Lambda = 1$, $\bar{\chi}_{e1} = \bar{\chi}_{e2} = 0{\cdot}01$

	Rigid body			Flexible body ($u = 0.7$)		
	Zeroth mode		First mode	Zeroth mode		First mode
f_2	Ω_1	Ω_2	Ω_3	Ω_1	Ω_2	Ω_3
1·0	0 + i1·955 (0 + i1·956)	0 − i0·757 (0 − i0·761)	0·583 − i0·356 (0·582 − i0·356)	0 + i1·934 (0 + i1·934)	0 − i0·735 (0 − i0·735)	0·584 − i0·347 (0·584 − i0·348)
0·8	0 + i1·946 (0 + i1·949)	0 − i0·304 (0 − i0·301)	0·835 − i0·390 (0·836 − i0·392)	0 + i1·931 (0 + i1·931)	0 − i0·292 (0 − i0·292)	0·833 − i0·375 (0·833 − i0·376)
0·4	0 + i1·958 (0 + i1·961)	0 − i0·084 (0 − i0·084)	1·144 − i0·202 (1·146 − i0·203)	0 + i1·947 (0 + i1·947)	0 − i0·087 (0 − i0·087)	1·136 − i0·189 (1·136 − i0·190)
0·0	0 + i2·031 (0 + i2·034)	0 + i0·423 (0 + i0·424)	1·279 − i0·014 (1·281 − i0·015)	0 + i2·023 (0 + i2·023)	0 + i0·419 (0 + i0·419)	1·273 − i0·004 (1·273 − i0·005)

Note: Analytical results from reference [3], recomputed using PSM. Present FE results are shown in the parenthesis.

TABLE 4

Numerical verification of stability criteria for a neutrally buoyant pinned–free string in axial flow by FEM: $L = 1$ m, $D = 0.05$ m

		ω (rad/s)		
εc_f	U (m/s)	$f_2 = 0{\cdot}8$, $c_{b2} = 0$ (Tapered end)	$f_2 = 0{\cdot}2$, $c_{b2} = 0{\cdot}8$ (Blunt end)	$T_0 = MU^2$ (Blunt end)
1	1	0 − i1·1003 1·1678 − i1·1062	0 − i0·5087 6·9042 − i0·6080	0·6613 + i0·3986 1·9866 + i0·4049
	3	0 − i3·3009 3·4463 − i33·2992	0 − i1·5262 12·7311 − i1·0844	2·2386 + i1·2322 6·7203 + i1·2485
1·5	1	0 − i0·8265 12·3226 − i5·8014	0 − i0·5087 6·9042 − i0·6080	— —
	3	0 − i2·4793 15·5771 − i2·3263	0 − i1·5262 12·7311 − i1·0844	2·4283 + i1·4371 7·3215 + i1·4661
2·05	1	0 − i0·2588 8·4180 − i9·1079	0 + i0·9280 5·1112 + i6·1696	—
	3	0 − i0·8006 6·4408 − i1·1882	0 + i4·0696 9·5351 + i9·8320	—

7. APPLICATION TO SHIP-TOWED CABLE–ARRAY SYSTEM

In this section, an important practical problem of ship-towed neutrally buoyant instrumented array module attached to a negatively buoyant tow cable is considered using the finite element code developed. In many practical situations, a tail rope or a drogue is

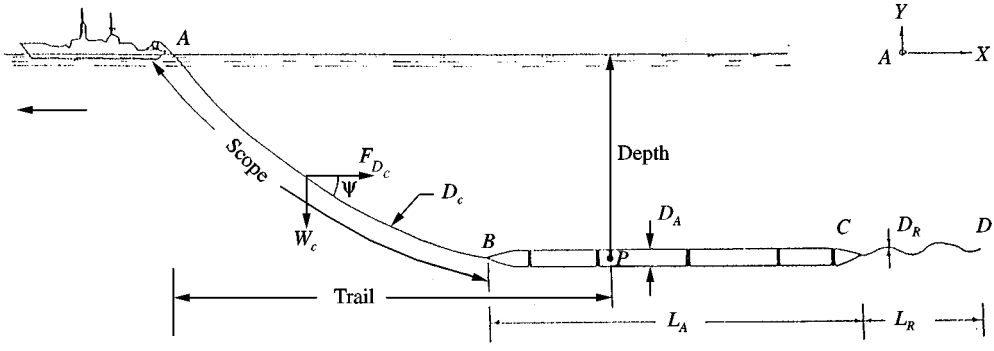

Figure 5. Definition sketch of a ship towed array system.

attached to the free end of the array to reduce the undulation or "snaking" motion. This aspect is also studied. Attempt is made to investigate the stability of the towed array system under constant tow speed by examining its free modes that grow or decay with time. The critical tow speed of this system is predicted, which is the most important information required for the operation of such a system. Such a practical structure cannot be handled by analytical methods because of the variability of the structural and the hydrodynamic parameters of different modules making up the array and the curved equilibrium configuration of a ship-towed array. The finite element method is therefore ideally suited for such problems.

A definition sketch of a towed cable-array system is schematically shown in Figure 5. The segment AB is the tow cable of diameter D_C, the segment BC is the towed array of diameter D_A followed by the segment CD which is a tail rope of diameter D_R. Consider a point P on the system. It can be located either on the cable or on the array. The vertical and horizontal distances of point P from A are called depth and trail of the point P respectively. The tail rope at the downstream end of the module provides certain magnitude of tension to keep the array free from "snaking".

The steady state tow configuration of this system has been obtained by a finite element analysis using a beam/cable element. This involves the equilibrium of hydrodynamic, hydrostatic, inertial and elastic forces acting on various parts of the system for a given ship tow speed. This analysis also provides the axial force of the towed cable–array system along their lengths, which serve as input for the stability analysis. The steady state configuration obtained for each tow speed can be analyzed using the FE code to assess its stability.

In this study, a typical towed array system has been chosen whose physical properties are given in Table 5. The towed system is assumed to be fixed at the onboard winch and free at its downstream end. The free end is assumed to be streamlined with parameters $f_2 = 1$ and $c_{b2} = 0$. The assumption of a streamlined end is consistent with the operational requirement of minimum flow noise in such systems. The steady state configuration was obtained for a few selected operating tow speeds and typical set of results is shown in Figure 6. For example, Figure 6(a) gives the operating depth versus the trail distance for a system as well as the axial force (i.e., tension) distribution along its length for four values of tow speeds in the operational range. It may be seen that the depth of operation varies form 10 to 29 m in this speed range. The axial force is an important parameter in the design of winch. It may be seen that the axial force varies between 3 and 15 kN in the speed range considered. The critical angles of tow for 8, 12, 16 and 20 knots (1 knot = 0·5144 m/s) were obtained as 19, 13, 10 and 8° respectively. The stability results are also given in Table 5 showing that as the

TABLE 5

Stability behaviour of ship towed array system

Cable scope (m)	Length of array (m)	Tow speed (knots)			
		8	12	16	20
100	150	S	S	D	D
500	150	S	S	S	S

Notes: 1. D—Divergence, S—stable.
2. Diameter of cable and array are 0·032 and 0·088 m respectively.
3. Mass per unit length of cable and array are 39·84 and 61·22 N/m respectively.
4. Submerged weight of cable and array are 31·75 and 0 N/m respectively. The array is neutrally buoyant.
5. Normal drag coefficient of cable and array are 1 and 0·8 respectively.
6. Tangential drag coefficient of cable and array are 0·015 and 0·0025 respectively.
7. Young's modulus (E) of cable and array are $0{\cdot}45 \times 10^{11}$ and $0{\cdot}08 \times 10^{11}$ N/m^2 respectively.

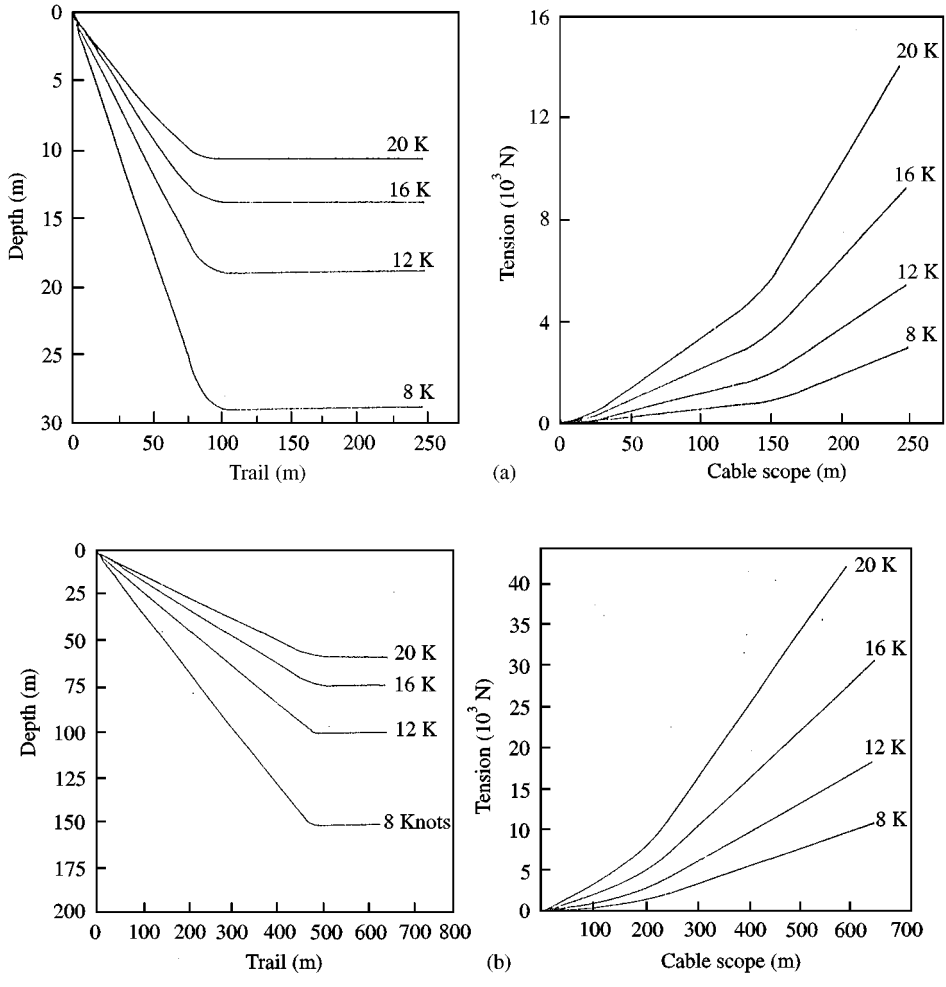

Figure 6. Tow curves of ship towed array systems: (a) cable scope = 100 m, array length = 150 m; (b) cable scope = 500 m, array length = 150 m.

speed increases, the system with 100 m cable scope becomes unstable by divergence in the speed range of $12 < U < 16$ knots, whereas the system with much longer cable scope (500 m) remains stable in the entire speed range considered. For a desired operating depth, the parameters of cable scope and tow speed can therefore be selected from such analysis so as to avoid instability.

8. CONCLUSION

A comprehensive finite element method has been developed for "towed cylinders in axial flow" problems for the first time. This is useful in predicting various instabilities, which occur in underwater towing of flexible cylindrical structures. The Hamilton's principle for such a non-conservative system is developed comprehensively for the first time. The finite element approximation is developed based on Hamilton's principle. A computer code has been implemented and several validation examples worked out showing "almost exact" performance of the method. Convergence properties of the method have been studied and practical modelling recommendations suggested. The developed code has been employed to study an example problem of underwater towing by ships. In doing this, various practical aspects of the problem are looked into, thereby demonstrating the versatility of the method.

REFERENCES

1. S. S. CHEN 1988 *Flow-Induced Vibration of Circular Cylindrical Structures*. Berlin: Springer-Verlag.
2. M. P. PAIDOUSSIS 1987 *Applied Mechanics Review* **40**, 163–175. Flow-induced instabilities of cylindrical structures.
3. M. P. PAIDOUSSIS 1970 *Eighth Symposium of Naval Hydrodynamics*: *Hydrodynamics in the Ocean Environment*, *ACR*-179, *Arlington Virginia*, 981–1016. Dynamics of submerged towed cylinders.
4. G. S. TRIANTAFYLLOU and C. CHRYSSOSTOMIDIS 1985 *Journal of Energy Resources Technology* **107**, 421–425. Stability of a string in axial flow.
5. C. R. ORTLOFF and J. IVES 1969 *Journal of Fluid Mechanics* **38**, 713–720. On the dynamic motion of a thin flexible cylinder in a viscous stream.
6. C. P. VENDHAN, S. K. BHATTACHARYYA and K. SUDARSAN 1997 *Journal of Sound and Vibration* **208**, 587–601. Stability characteristics of slender flexible cylinders in axial flow by finite element method.
7. R. S. BARSOUM 1971 *International Journal for Numerical Methods in Engineering* **3**, 63–87. Finite element method applied to the problem of stability of a non-conservative system.
8. C. D. MOTE 1971 *Journal of Engineering Mechanics Division*, *ASCE* **97**, 645–656. Non-conservative stability by finite element.
9. W. H. CHEN and C. N. FAN 1987 *Journal of Sound and Vibration* **119**, 429–442. Stability analysis with lumped mass and friction effects in elastically supported pipes conveying fluids.
10. A. PRAMILLA, J. LAUKKANEN and S. LIUKKONEN 1991 *Journal of Sound and Vibration* **144**, 421–425. Dynamics and stability of short fluid-conveying Timoshenko element pipes.
11. M. KANGASPUOSKARI, J. LAUKKANEN and A. PRAMILA 1993 *Journal of Fluids and Structures* **7**, 707–715. The effect of feedback control on critical velocity of cantilevered pipes aspirating fluid.
12. M. J. LIGHTHILL 1970 *Journal of Fluid Mechanics* **44**, 265–301. Aquatic animal propulsion of high hydromechanical efficiency.
13. G. I. TAYLOR 1952 *Proceedings of Royal Society* (*London*) **A-214**, 158–183. Analysis of the swimming of long and narrow animals.
14. T. Y. YANG 1986 *Finite Element Structural Analysis*. NJ: Prentice-Hall.
15. M. P. PAIDOUSSIS 1973 *Journal of Sound and Vibration* **29**, 365–385. Dynamics of cylindrical structures subjected to axial flow.

APPENDIX A. POWER SERIES METHOD

Following the presentation in reference [6], the non-dimensional differential equation in space co-ordinates $\xi[Y = Y(\xi)]$ is written as

$$Y'''' + aY'' + b\xi Y'' + cY' + eY = 0 \quad (0 < \xi < 1), \tag{A1}$$

where a, b, c and e are constant coefficients and $Y' = \mathrm{d}Y/\mathrm{d}\xi$, etc. The boundary conditions are

clamped–free:

$$Y = Y' = 0 \quad \text{at } \xi = 0, \qquad Y'' = Y''' + jY' + pY = 0 \quad \text{at } \xi = 1, \tag{A2}$$

towed–free:

$$Y'' = Y''' + j_1 Y' + p_1 Y = 0 \quad \text{at } \xi = 0, \qquad Y'' = Y''' + j_2 Y' + p_2 Y = 0 \quad \text{at } \xi = 1. \tag{A3}$$

The solution of equation (A1) is assumed as

$$Y(\xi) = \sum_{n=0}^{\infty} A_n \xi^n. \tag{A4}$$

The various required derivatives are

$$Y' = \sum_{n=0}^{\infty} nA_n \xi^{n-1}, \qquad Y'' = \sum_{n=0}^{\infty} n(n-1) A_n \xi^{n-2}, \qquad Y''' = \sum_{n=0}^{\infty} n(n-1)(n-2) A_n \xi^{n-3}. \tag{A5}$$

Use of equations (A2)–(A4) gives

clamped–free:

$$A_0 = A_1 = 2A_2 + 6A_3 + \sum_{n=4}^{\infty} n(n-1) A_n = (2j + p) A_2 + (6 + 3j + p) A_3$$

$$+ \sum_{n=4}^{\infty} [n(n-1)(n-2) + nj + p] A_n = 0, \tag{A6}$$

towed–free:

$$A_2 = 6A_3 + j_1 A_1 + p_1 A_0 = 6A_3 + \sum_{n=4}^{\infty} n(n-1) A_n = 6A_3 + \sum_{n=4}^{\infty} n(n-1)(n-2) A_n$$

$$+ j_2 A_1 + 3j_2 A_3 + j_2 \sum_{n=4}^{\infty} nA_n + p_2 (A_0 + A_1 + A_3) + p_2 \sum_{n=4}^{\infty} A_n = 0. \tag{A7}$$

Subsituting equation (A4) into equation (A1) and collecting terms of like powers of ξ, one obtains

$$n(n-1)(n-2)(n-3) A_n + a(n-2)(n-3) A_{n-2}$$

$$+ [b(n-3)(n-4) + c(n-3)] A_{n-3} + eA_{n-4} = 0. \tag{A8}$$

One writes this relation as

$$A_n = f_{1n}A_{n-2} + f_{2n}A_{n-3} + f_{3n}A_{n-4}, \tag{A9a}$$

where

$$f_{1n} = -\frac{a}{n(n-1)}, \qquad f_{2n} = -\frac{b(n-3)(n-4) + c(n-3)}{n(n-1)(n-2)(n-3)},$$

$$f_{3n} = -\frac{e}{n(n-1)(n-2)(n-3)}. \tag{A9b–d}$$

In view of equation (A8), one obtains for various cases,

clamped–free:

$$A_n = G_n A_2 + H_n A_3, \tag{A10a}$$

towed–free:

$$A_n = F_n A_0 + G_n A_1 + H_n A_3, \tag{A10b}$$

where for clamped–free case upto $n = 3$

$$G_2 = H_3 = 1, \qquad G_1 = H_1 = H_2 = G_3 = 0, \tag{A11a}$$

and for towed–free case upto $n = 4$

$$F_0 = G_1 = H_3 = 1, \qquad F_1 = F_2 = F_3 = G_0 = G_2 = G_3 = H_0 = H_1 = H_2 = 0, \tag{A11b}$$

Using equations (A10a) or equation (A10b) in equation (A9a) one obtains

$$G_n = f_{1n}G_{n-2} + f_{2n}G_{n-3} + f_{3n}G_{n-4}, \tag{A12a}$$

$$H_n = f_{1n}H_{n-2} + f_{2n}H_{n-3} + f_{3n}H_{n-4}. \tag{A12b}$$

$$F_n = f_{1n}F_{n-2} + f_{2n}F_{n-3} + f_{3n}F_{n-4}. \tag{A12c}$$

Using these recursive relations in equations (A6), (A7) and (A11) in conjunction with either equation (A10a) or equation (A10b), one obtains a system of equations

$$[a_{ij}]\{B_j\} = \{0\}, \tag{A13}$$

where for a clamped–free cylinder

$$B_1 = A_2, \qquad B_2 = A_3, \qquad a_{11} = 2 + \sum_{n=4}^{\infty} n(n-1)G_n, \qquad a_{12} = 6 + \sum_{n=4}^{\infty} n(n-1)H_n,$$

$$a_{21} = 2j + p + \sum_{n=4}^{\infty} [n(n-1)(n-2) + nj + p]G_n,$$

$$a_{22} = 6 + 3j + p + \sum_{n=4}^{\infty} [n(n-1)(n-2) + nj + p]H_n \tag{A14a}$$

and for a towed–free cylinder

$$B_1 = A_0, \qquad B_2 = A_1, \qquad B_3 = A_3, \qquad a_{11} = \sum_{n=4}^{\infty} n(n-1)F_n, \qquad a_{12} = \sum_{n=4}^{\infty} n(n-1)G_n,$$

$$a_{21} = p_1, \qquad a_{22} = j_1, \qquad a_{23} = 6, \qquad a_{31} = p_2 + \sum_{n=4}^{\infty} [n(n-1)(n-2) + nj_2 + p_2]F_n,$$

$$a_{32} = p_2 + j_2 + \sum_{n=4}^{\infty} [n(n-1)(n-2) + nj_2 + p_2]G_n,$$

$$a_{33} = 6 + 3j_2 + p_2 + \sum_{n=4}^{\infty} [n(n-1)(n-2) + nj_2 + p_2]H_n. \tag{A14b}$$

For non-trivial solution one requires

$$f(\Omega) = |a_{ij}| = 0. \tag{A15}$$

The number of terms (n) in equation (A4) determines the convergence of roots of equation (A15). However, since the root computation of this 2×2 or 3×3 determinantal equation is extremely fast in computer, a large n makes little difference in computer time. In all calculations, typically $n = 100$ have been used, which is a sufficiently high value for all cases for accurate convergence.

APPENDIX B: NOMENCLATURE

A	cross-sectional area of cylinder
$A(x)$	cross-sectional area over length of taper
C_D	normal drag coefficient
C_{b1}, C_{b2}	coefficients of base drag at upstream and downstream ends respectively
C_N, C_T, C_f	coefficients of normal, tangential and frictional drag respectively
$\langle C_N, C_T, C_f, C_{b1}, C_{b2}\rangle$	$= \langle c_N, c_T, c_f, c_{b1}, c_{b2}\rangle \pi/4$
D	outer diameter of cylinder
E	Young's modulus of cylinder material
F_A	fluid inertial force per unit length on cylinder in the $-y$ direction
F_N, F_T	normal and tangential viscous forces per unit length on cylinder respectively
f_1, f_2	shape coefficients at upstream and downstream ends respectively
I	moment of inertia of cylinder cross-section about centroidal axis
L	length of cylinder
l_1, l_2	short lengths of taper at upstream and downstream ends respectively
M	added mass per unit length of cylinder
$\bar{M}$	sectional bending moment
m	mass per unit length of cylinder
$\bar{m}_i$	sum of structural mass and hydrodynamic added mass of tapered end i (= 1: upstream, = 2: downstream)
$\mathrm{N_i}$	beam shape functions
P	tow rope pull
Q	sectional shear force
Q_i	generalized beam element forces corresponding to u_i
s	tow rope length at upstream end
T	Axial tension on cylinder
T_0	Initial tension on cylinder
T_{b1}, T_{b2}	base or form drag at upstream and downstream (free) ends respectively
T_E	externally imposed end tension at free downstream end of cylinder

$\bar{T}$	total kinetic energy of system
$\bar{T}_1$	kinetic energy of structural mass
$\bar{T}_2$	kinetic energy due to M associated with total transverse velocity
$\bar{T}_3$	kinetic energy of lumped mass at ends due to taper
t	time
t_1, t_2	instances of t at which system configurations are known
U	tow speed (or constant flow velocity along cylinder axis)
u_i	degrees of freedom of beam element
v	transverse displacement of cylinder (in the y direction)
$\bar{V}$	potential energy of the system, which includes strain energy and potential of conservative external forces
$\bar{V}_1$	bending strain energy of beam
$\bar{V}_2$	potential energy due to action of axial force and rotation of beam
$\delta \bar{W}_{nc}$	virtual work done by non-conservative forces (not included in $\bar{V}$)
x, y	co-ordinate system with x as undeformed centroidal axis of horizontal cylinder
$\bar{x}, \bar{y}$	beam local co-ordinate system
ρ	fluid density
ϕ	angle of incidence
γ	$= 0$ (end free to slide axially), $= 1$ (supported end, no axial stretching)
ε	slenderness ratio of (L/D) of cylinder
δ	symbol for variation
μ	nondimensional tow speed $(= UL\sqrt{M/EI})$
β	mass ratio of cylinder $(= M/(m + M))$
Λ	nondimensional tow rope length $(= s/L)$
ω	circular frequency
Ω	nondimensional frequency $(= \omega L^2\sqrt{(M + m)/EI})$
$\bar{\chi}_{ei}$	nondimensional effective length of taper $(= \chi_{ei}/L)$, see Equation (15), at upstream $(i = 1)$ and downstream $(i = 2)$ ends